Current Biomedicine
p-ISSN: 2962-8490; e-ISSN: 2985-4784
https://journal.ipb.ac.id/index.php/currbiomed

Tsurumoto
Vol 5 No 1, January 2027, Pp 1–6
DOI: 10.29244/currbiomed.5.1.1

Short communication **OPEN ACCESS**

Preliminary comparison of respiratory rate estimation methods using simultaneous dual-position under-mattress millimeter-wave radar

Masanobu Tsurumoto*

Department of Clinical Engineering, Faculty of Health and Welfare, Tokushima Bunri University, Takamatsu, Kagawa 760-8542, Japan

Abstract

Background Under-mattress millimeter-wave radar may provide unobtrusive respiratory sensing, but signal morphology can vary with sensor position and estimation method. This study aimed to compare frequency-domain and time-domain respiratory rate estimation using simultaneous dual-position under-mattress radar measurements.

Methods Three healthy adult volunteers underwent supine instructed breathing at 10, 12, and 15 breaths/min. Two XM125 60-GHz-class radar modules were operated simultaneously beneath an 8-cm non-coil medical mattress at positions aligned with the sternal angle and xiphoid process. Each condition was repeated three times, yielding 27 paired trials and 54 radar recordings. The respiratory rate was estimated using a power spectral density method and time-domain peak detection. Mean absolute error, root mean square error, paired position differences, and exploratory harmonic characteristics of peak-detection failures were examined.

Results Estimation based on power spectral density yielded a mean absolute error of 0.472 breaths/min and a root mean square error of 0.479 breaths/min, compared with 1.710 and 2.250 breaths/min for peak detection. The mean paired difference between sensor positions was +0.037 breaths/min for power spectral density estimation and +0.164 breaths/min for peak detection. Power spectral density estimates differed by no more than 0.05 breaths/min in 26 of 27 paired trials. Recordings with peak-detection errors greater than 1.0 breaths/min showed higher second- and third-harmonic ratios.

Conclusion Under controlled instructed-breathing conditions, power spectral density-based estimation showed smaller deviations from the instructed breathing rates than simple peak detection, whereas the two positions generally yielded similar frequency-domain estimates. These findings are technical results relative to instructed breathing rates and do not constitute clinical validation.

Keywords millimeter-wave radar | non-contact monitoring | power spectral density | respiratory rate | under-mattress sensing

Introduction

Respiratory rate is a fundamental physiological parameter used in clinical observation, sleep assessment, and bed-based monitoring. Conventional methods such as visual counting, respiratory belts, impedance pneumography, and airflow sensing can provide useful measurements but often require direct contact with the patient or visible attachment of sensors (Nicolò *et al.,* 2020; Bawua *et al.,* 2021). Unobtrusive sensing methods may therefore be useful when continuous monitoring with minimal behavioral interference is desired.

Radar-based respiratory sensing detects small motions associated with breathing without attaching a transducer to the body. Previous studies have demonstrated non-contact respiratory or cardiorespiratory monitoring using radar posi-

***Corresponding author** Email: tsurumoto@kgw.bunri-u.ac.jp

©The Author(s) 2026 This article is licensed under a Creative Commons Attribution (CC BY 4.0) International License, which permits use, sharing, adaptation, distribution, and reproduction in any medium or format, as long as you give appropriate credit to the original author(s) and the source, and indicate if changes were made.

tioned near the body or bed (Sun *et al.,* 2019; Schellenberger *et al.,* 2020; Lv *et al.,* 2021; Edanami & Sun, 2022). A radar installed beneath a mattress is particularly attractive because the sensor can be integrated into the bed structure and remain out of the user's way; however, the measured signal may be affected by the mattress, dorsal body contact, body-weight distribution, local mechanical coupling, and sensor alignment (Otake *et al.,* 2021; Tamura & Huang, 2025).

These constraints raise two practical questions. First, it is unclear whether under-mattress positions aligned with different thoracoabdominal landmarks provide comparable respiratory-rate information when measured simultaneously. Second, waveform distortion or local secondary peaks may affect simple time-domain peak counting differently from frequency-domain estimation. The present research note therefore evaluated respiratory-rate estimation from two simultaneously operated under-mattress millimeter-wave radar sensors. The primary objective was to compare estimation based on power spectral density (PSD) with time-domain peak detection relative to instructed breathing rates. The secondary objective was to describe paired differences between two sensor positions. An exploratory harmonic analysis was used to examine recordings with large peak-detection errors. This study was designed as a technical feasibility and method-comparison evaluation rather than a clinical validation study.

Methods

Experimental setup and data acquisition

The study was approved by the Ethics Committee of Tokushima Bunri University (R8-9; May 1, 2026), and informed consent was obtained from all participants. Data were collected from 27 to 29 May 2026 at the Department of Clinical Engineering, Tokushima Bunri University, Takamatsu, Japan. Three healthy adults (one male and two females; all aged 21 years) participated in the study. Their heights ranged from 160 to 165 cm, and their mean body weight was 50 kg.

The experimental configuration is illustrated in **Figure 1**. Each participant lay supine on a medical bed manufactured by Paramount Bed Co., Ltd. (Japan). An 8-cm-thick Paramount Bed PREGLAR non-coil medical mattress was used. Two XM125 millimeter-wave radar modules (Acconeer AB, Sweden), each equipped with an A121 60-GHz-class pulsed coherent radar sensor, were fixed beneath the mattress and oriented upward toward the participant's dorsal surface. Sensor 1 was aligned with the region corresponding to the sternal angle (angle of Louis), and Sensor 2 was aligned with the region corresponding to the xiphoid process.

For each participant, the mattress positions corresponding to these anatomical landmarks were identified and marked with adhesive tape. The mattress was kept fixed in position during each measurement to prevent displacement of the marked locations, and the radar modules were secured beneath the mattress so that the center of each sensor was aligned with the corresponding mark. Because the sensor positions were adjusted individually according to each participant's anatomical landmarks, the center-to-center distance between Sensor 1 and Sensor 2 ranged from 8 to 10 cm.

Data acquisition from both radar modules was controlled by a custom Python-based application running on a single Windows laptop computer. The application initiated and terminated acquisition from both sensors within the same measurement session, allowing simultaneous dual-position recording. Overlap of the recording intervals was checked using the PC timestamps stored in the CSV files. These timestamps document temporal correspondence at the PC-recording level but do not establish exact synchronization of

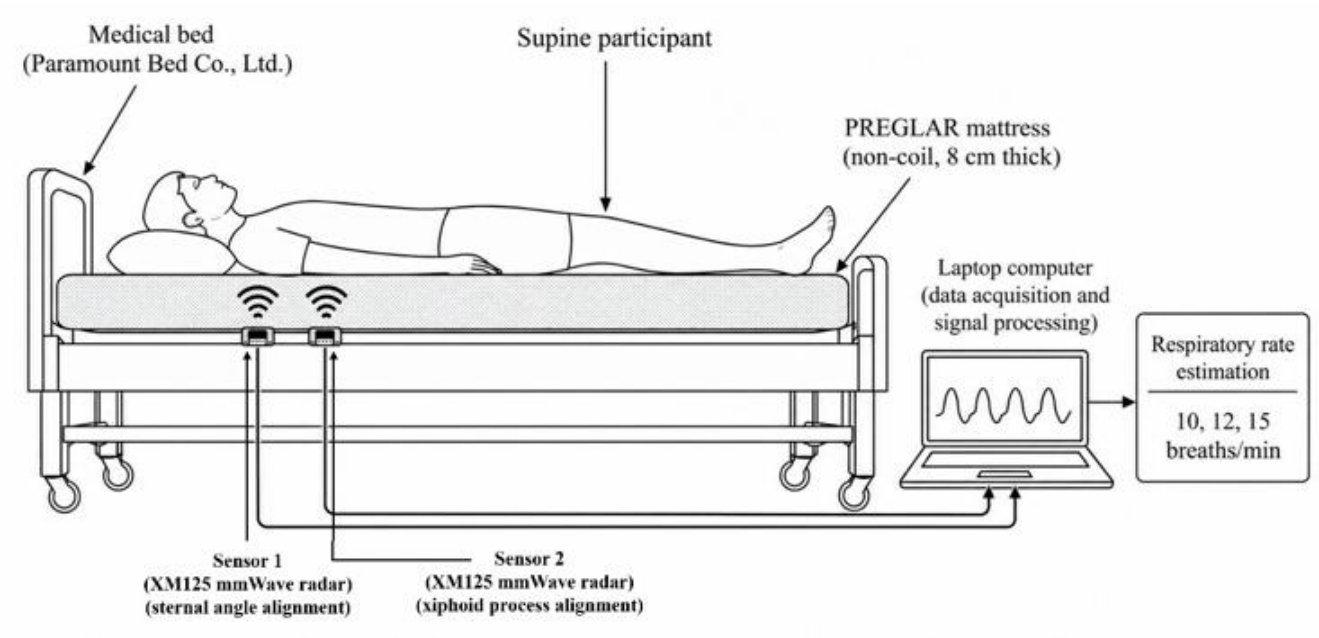


Figure 1 Experimental setup for the simultaneous dual-position under-mattress millimeter-wave radar measurement. Two XM125 radar modules were positioned beneath an 8-cm-thick PREGLAR non-coil medical mattress and aligned with the sternal-angle (Sensor 1) and xiphoid-process (Sensor 2) regions. The sensors were operated simultaneously during supine instructed breathing at 10, 12, and 15 breaths/min.

sensor acquisition times. The sensors did not contact the participant.

The participants were instructed to breathe at 10, 12, and 15 breaths/min using auditory counting cues played through a speaker. The cues provided an audible count of elapsed seconds, and participants were instructed to complete one respiratory cycle at intervals corresponding to the target breathing rate (6, 5, and 4 s per cycle for 10, 12, and 15 breaths/min, respectively). The participants practiced the paced-breathing procedure before data acquisition.

Each breathing condition was repeated three times, and each recording lasted approximately 60 s. The resulting dataset comprised 27 simultaneous paired trials (3 participants × 3 instructed rates × 3 repetitions) and 54 radar recordings (27 trials × 2 sensors). The instructed breathing rate was used as the comparison value; no independent physiological respiratory reference device was used.

Signal processing and range-bin selection

Each recording contained 80 range-bin signals and was sampled at approximately 20.8 Hz. The sampling frequency for each file was calculated from the median inter-sample interval recorded in the timestamp data. The entire recording interval was analyzed. For each range bin, the signal was linearly detrended before Welch power spectral density (PSD) estimation. Welch PSD was calculated using a Hann window, segment duration of up to 60 s, 50% overlap, FFT length equal to the segment length, and linear detrending within each segment. A respiratory band of 0.08–0.50 Hz (4.8–30 breaths/min) was applied. For range-bin selection, the respiratory-band power, fraction of total spectral power contained within the respiratory band, and ratio of the dominant respiratory-band peak to the median respiratory-band power were calculated.

The quality score was defined as the product of the latter two quantities, and the single range bin with the highest quality score was selected. The instructed breathing rate was not used for range-bin selection. Because no single range bin was predefined as the respiratory-signal bin, an automated criterion independent of the instructed breathing rate was required to select a common signal for both estimation methods. Therefore, a frequency-domain criterion was used rather than a time-domain peak-based criterion because peak morphology was evaluated by the peak-detection method, and using it for range-bin selection could have favored that method.

Respiratory rate estimation and performance analysis

The dominant Welch-PSD frequency within 0.08–0.50 Hz was converted to breaths/min for PSD-based estimation. The same selected range-bin signal was linearly detrended and filtered with a third-order zero-phase Butterworth band-pass filter over 0.08–0.50 Hz for time-domain peak detection. Peaks were detected with a minimum spacing corresponding to 30 breaths/min and a prominence threshold of 0.25 times the standard deviation of the filtered signal. The respiratory rate was calculated from the number of inter-peak intervals divided by the elapsed time from the first to the last detected peak.

Estimation error was calculated relative to the instructed breathing rate, for both methods. The overall performance was summarized by mean absolute error (MAE) and root mean square error (RMSE). Because the two sensors were recorded simultaneously, between-position differences were described using the paired difference:

$$\Delta RR = RR_{Sensor\ 1} - RR_{Sensor\ 2}$$

ΔRR: paired difference in respiratory rate,
$RR_{Sensor\ 1}$: respiratory rate estimated from Sensor 1,
$RR_{Sensor\ 2}$: respiratory rate estimated from Sensor 2.

The paired differences were reported as the mean, median, and standard deviation (SD) of 27 paired trials. Given the small number of participants and the repeated-measures structure, the between-position analysis was descriptive, and no inferential test of sensor-position superiority was prespecified.

Exploratory harmonic analysis

Recordings were classified according to whether the absolute peak-detection error was ≤1.0 or >1.0 breaths/min as an exploratory failure-case analysis. The maximum PSD was identified separately within ±1.0 breaths/min of the instructed fundamental frequency and of its second and third harmonics using the full Welch spectrum of the selected range bin. Second- and third-harmonic ratios were calculated relative to the maximum PSD near the fundamental. This post-hoc analysis was used only to characterize peak-detection failure patterns and not to establish causality. Data processing and analyses were performed using Python 3.12.4, NumPy 1.26.4, pandas 2.2.2, and SciPy 1.13.1.

Results

All 54 radar recordings were included. PSD-based estimation showed smaller deviations from the instructed breathing rates than peak detection. PSD-based estimation yielded an MAE of 0.472 breaths/min and an RMSE of 0.479 breaths/min, whereas peak detection yielded an MAE of 1.710 breaths/min and an RMSE of 2.250 breaths/min. Position-specific PSD MAEs were 0.471 breaths/min at the sternal-angle-aligned position and 0.474 breaths/min at the xiphoid-process-aligned position. The corresponding peak-detection MAEs were 1.799 and 1.621 breaths/min, respectively (**Table 1**).

The absolute difference between the two positions was ≤0.05 breaths/min in 26 of 27 paired trials for PSD-based estimation. One paired trial during instructed breathing at 12 breaths/min showed a larger positional difference of approximately 1.03 breaths/min. Thus, the two positions generally provided similar dominant-frequency estimates under the present controlled conditions, but complete position invariance was not observed. Peak detection showed substantially greater between-position variability, as reflected by an SD of 1.683 breaths/min for paired differences.

Table 1 Respiratory-rate estimation and paired position differences

Outcome	PSD-based	Peak detection
Recordings, n	54	54
Overall MAE, breaths/min	0.472	1.710
Overall RMSE, breaths/min	0.479	2.250
Sensor 1 MAE, breaths/min	0.471	1.799
Sensor 2 MAE, breaths/min	0.474	1.621
Paired trials, n	27	27
Sensor 1–Sensor 2 mean difference, breaths/min	+0.037	+0.164
Sensor 1–Sensor 2 median difference, breaths/min	0.000	+0.191
SD of paired difference, breaths/min	0.198	1.683

Sensor 1: sternal-angle-aligned position; Sensor 2: xiphoid-process-aligned position. Paired difference was defined as Sensor 1 minus Sensor 2. PSD: power spectral density; MAE: mean absolute error; RMSE: root mean square error; SD: standard deviation.

The exploratory harmonic analysis classified 24 recordings as having peak-detection absolute error ≤1.0 breaths/min and 30 recordings as having error >1.0 breaths/min. The mean second-harmonic ratio was 0.060 in the smaller-error group and 0.132 in the larger-error group; the corresponding mean third-harmonic ratios were 0.012 and 0.038. In the largest peak-detection error example, the instructed breathing rate was 10 breaths/min, the peak-detection estimate was 16.82 breaths/min, and the PSD-based estimate was 10.38 breaths/min. A second-harmonic component was visible near 20 breaths/min (**Figure 2**). These observations were descriptive and exploratory.

Discussion

This preliminary technical study revealed three main findings. First, respiratory rate-related information could be obtained simultaneously from two under-mattress radar positions through an 8-cm non-coil medical mattress during instructed supine breathing. Second, within the preprocessing pipeline used in this study, PSD-based estimation showed smaller deviations from the instructed rates than simple time-domain peak detection. Third, PSD-derived respiratory-rate estimates showed small differences between the two evaluated positions in 26 of 27 paired trials, whereas peak detection showed greater between-position variability.

The present findings are consistent with previous reports demonstrating non-contact respiratory monitoring using radar; however, direct numerical comparison is limited by differences in radar configuration, sensor placement, and reference methods (Schellenberger *et al.,* 2020; Lv *et al.,* 2021; Edanami & Sun, 2022).

The difference between estimation methods is technically plausible. Under-mattress sensing does not directly measure anterior thoracoabdominal displacement; instead, the radar signal may reflect dorsal body-surface movement and mattress-mediated mechanical motion (Otake *et al.,* 2021; Tamura & Huang, 2025). Therefore, a single respiratory cycle can contain waveform asymmetry, local fluctuations, or multiple time-domain peaks. Frequency-domain estimation can remain centered on the dominant periodic component even when waveform morphology is irregular, whereas simple peak detection may count secondary local peaks. The largest peak-detection failure case and exploratory harmonic analysis were consistent with this interpretation, because recordings with larger peak-detection errors showed higher second- and third-harmonic ratios. These harmonic components may arise from nonsinusoidal respiratory motion and mattress-mediated mechanical coupling, which can introduce repeated waveform structure within a single respiratory cycle.

In the representative 10 breaths/min case, the second and third harmonics occurred at approximately 0.33 and 0.50 Hz, respectively, which are below the typical fundamental cardiac-frequency range reported for radar-based vital-sign monitoring (Schellenberger *et al.,* 2020). Moreover, the time-domain analysis in this study used a 0.08–0.50 Hz band-pass filter, placing the typical cardiac fundamental component outside the analyzed frequency band. Nevertheless, higher-order respiratory harmonics can extend toward the cardiac-frequency range, and no independent cardiac reference signal was recorded in this study. Therefore, a contribution from cardiac-related motion cannot be completely excluded, although it is unlikely to explain the second- and third-harmonic components highlighted in the representative case. However, these findings do not establish that harmonic components caused the peak-detection errors.

The simultaneous design provides a useful paired assessment of position effects because both sensors observed the same instructed breathing trial. The near-zero median PSD difference and the finding that 26 of 27 paired trials differed by no more than 0.05 breaths/min suggest that both evaluated positions generally contained similar dominant respiratory-frequency information under these controlled conditions. The single larger PSD position difference also indicates that sensor position, mechanical coupling, or local signal quality cannot be assumed to be irrelevant.

Several limitations require emphasis. Only three healthy volunteers were studied, all measurements were supine, and breathing was externally instructed at only 10, 12, and 15 breaths/min. The participants were also relatively homogeneous in body size, so the effect of body habitus on under-mattress radar recording could not be evaluated. Greater body mass or BMI could alter mattress compression, sensor-to-body geometry, and the mechanical transmission of respiratory motion, potentially affecting signal amplitude and waveform morphology. However, the present data cannot determine the direction of these effects, and it cannot be assumed that a higher BMI would reduce the harmonic components observed in the time-domain signal.

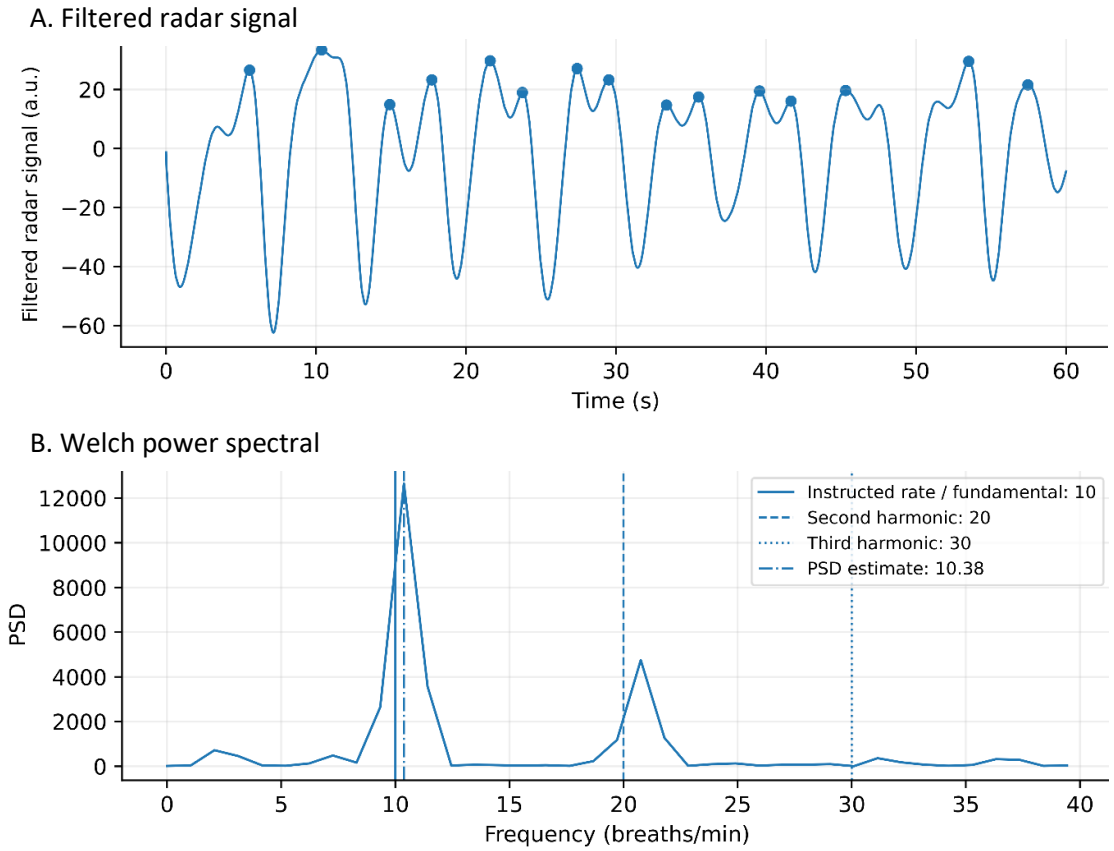


Figure 2 Representative peak-detection overestimation case during instructed breathing at 10 breaths/min. (**A**) Filtered radar signal in arbitrary units (a.u.) with detected peaks; the peak-detection estimate was 16.82 breaths/min. (**B**) Welch power spectral density; the PSD-based estimate was 10.38 breaths/min, and a second-harmonic component was visible near 20 breaths/min.

Because repeated recordings were obtained from the same three participants, the 54 recordings should not be interpreted as 54 independent biological observations. The instructed breathing rate was not an independent physiological reference measurement; therefore, the reported errors quantify deviation from the instructed rate and must not be interpreted as clinical measurement accuracy. Participants may not have followed the auditory metronome perfectly throughout each recording, and such deviations in actual breathing frequency could have contributed to the observed differences between the estimated and instructed rates. Accordingly, these differences cannot be attributed solely to algorithmic estimation errors in the absence of an independent physiological respiratory reference. Only one bed and one non-coil mattress configuration were examined.

Hardware-level synchronization between the two radar modules was not implemented. Although the recording intervals overlapped according to the PC timestamps, the exact offset between sensor acquisition times was not independently established. In addition, range-bin selection was based on a frequency-domain quality score. Consequently, the comparison between PSD estimation and peak detection describes estimator behavior after this common frequency-informed preprocessing step and should not be interpreted as an algorithm-independent head-to-head comparison. The harmonic analysis was post hoc and descriptive. Larger studies including participants across a broader range of body sizes and BMI, as well as spontaneous breathing, movement, different bedding conditions, and an independent respiratory reference device, are required before clinical performance can be assessed.

Conclusion

Simultaneous dual-position under-mattress millimeter-wave radar measurements were technically feasible during controlled supine instructed breathing. Within the present processing pipeline, PSD-based respiratory-rate estimation showed smaller deviations from instructed rates and greater consistency between the two evaluated positions than simple time-domain peak detection. Exploratory analysis suggested that local waveform structure and harmonic components may contribute to peak-detection overestimation. These results support further technical development but do not establish clinical respiratory-rate accuracy.

Acknowledgments Not applicable.

Funding This research received no external funding.

Conflict of interest The author declares no conflicts of interest in this research.

Author contribution M.T.: Conceptualization, methodology, software, formal analysis, investigation, resources, data curation, validation, visualization, project administra

tion, supervision, writing–original draft, and writing–review & editing.

Availability of data and materials The data supporting the findings of this study are available from the corresponding author upon reasonable request.

Declaration of generative AI in writing process During the preparation of this work, the author used ChatGPT (OpenAI) for limited assistance with manuscript organization and for checking analysis code. All study analyses, interpretation of results, and scientific conclusions were performed and verified by the author. Generative AI was not used to generate or alter the study data. The author reviewed all AI-assisted content and takes full responsibility for the content of the article.

Received 11 September 2026 | **Revised** 22 October 2026 | **Accepted** 26 October 2026 | **Published online** 10 November 2026

References

Bawua LK, Miaskowski C, Hu X, Rodway GW, Pelter MM. 2021. A review of the literature on the accuracy, strengths, and limitations of visual, thoracic impedance, and electrocardiographic methods used to measure respiratory rate in hospitalized patients. *Annals of Noninvasive Electrocardiology*, 26(5): e12885. DOI: 10.1111/anec.12885.

Edanami K, Sun G. 2022. Medical radar signal dataset for non-contact respiration and heart rate measurement. *Data in Brief*, 40: 107724. DOI: 10.1016/j.dib.2021.107724.

Lv W, He W, Lin X, Miao J. 2021. Non-contact monitoring of human vital signs using FMCW millimeter wave radar in the 120 GHz band. *Sensors*, 21(8): 2732. DOI: 10.3390/s21082732.

Nicolò A, Massaroni C, Schena E, Sacchetti M. 2020. The importance of respiratory rate monitoring: from healthcare to sport and exercise. *Sensors*, 20(21): 6396. DOI: 10.3390/s20216396.

Otake Y, Kobayashi T, Hakozaki Y, Matsui T. 2021. Non-contact heart rate variability monitoring using Doppler radars located beneath bed mattress: a case report. *European Heart Journal–Case Reports*, 5(8): ytab273. DOI: 10.1093/ehjcr/ytab273.

Schellenberger S, Shi K, Michler F, Lurz F, Weigel R, Koelpin A. 2020. Continuous in-bed monitoring of vital signs using a multi radar setup for freely moving patients. *Sensors*, 20(20): 5827. DOI: 10.3390/s20205827.

Sun G, Okada M, Nakamura R, Matsuo T, Kirimoto T, Hakozaki Y, Matsui T. 2019. Twenty-four-hour continuous and remote monitoring of respiratory rate using a medical radar system for the early detection of pneumonia in symptomatic elderly bedridden hospitalized patients. *Clinical Case Reports*, 7(1): 83–86. DOI: 10.1002/ccr3.1922.

Tamura T, Huang M. 2025. Unobtrusive bed monitor state of the art. *Sensors*, 25(6): 1879. DOI: 10.3390/s25061879.